Water response to ganglioside GM1 surface remodeling.

P. Brocca[a], V. Rondelli[a], V. Crupi[b], F. Mallamace[b], M.T. Di Bari[c], A. Deriu[c], W. Lohstroh[d], E. Del Favero[a], L. Cantu'[a], M. Corti[a]

[a]*Dept. of Medical Biotechnologies and Traslational Medicine, University of Milano, LITA, Via Fratelli Cervi, 93, 20090 Segrate (Italy)*

[b]*Dept. of Physics and Earth Sciences, University of Messina, Viale F. Stagno D'Alcontres, 31, 98166 Messina, Italy*

[c]*Dept. of Physics and Earth Sciences, University of Parma, Parco Area delle Scienze, 7/A, 23124 Parma, Italy*

[d]*Heinz Maier-Leibnitz Zentrum, Technische Universität München, Lichtenbergstraße 1, Garching, Germany*

Running title: Water structure modulation by GM1 ganglioside.

Keywords: gangliosides, sugar/water interactions, water structuring, Raman Scattering, Depolarized Rayleigh Scattering, OH-exchange rate, NMR.

*Corresponding author:

A. Deriu.....

ABSTRACT

Gangliosides are biological glycolipids participating in rafts, structural and functional domains of cell membranes. Their headgroups are able to assume different conformations when packed on the surface of an aggregate, more lying or standing. Switching between different conformations is possible, and is a collective event. Switching has been observed to be induced, in model systems, by concentration or temperature increase, then possibly involving ganglioside-water interaction. In the present paper, the effect of GM1 ganglioside heagroup conformation on the water structuring and interactions is addressed. Depolarized Rayleigh Scattering, Raman Scattering, Quasielastic Neutron Scattering and NMR measurements performed on GM1 ganglioside solutions indicate that both the structural properties of solvent water and its interactions with the sugar headgroups of GM1 respond to surface remodeling. The extent of this modification is much higher than expected and, interestingly, ganglioside headgroups seem to turn from cosmotropes to chaotropes. In a biological perspective, water structure modulation could be one of the physico-chemical elements contributing to the raft strategy.

Introduction

Gangliosides are natural amphiphilic multifunctional molecules of the class of glycosphingolipids.[1] They carry a quite long hydrophobic double tail, the ceramide, besides a large head group made up of several sugar rings. In that, they are far different from the other lipids, mainly phospholipids, with which they normally mix in membranes (see Fig.1 for the GM1 ganglioside structure and ganglioside nomenclature).

Gangliosides play a key role for recognition and transduction of membrane-mediated information.[2,3] They are known to participate in rafts and SEDs (Sphingolipid Enriched Domains), that is, structural and functional regions of membranes with high ganglioside density, involved in recognition processes, like antigen-antibody interaction.[4-6] Nevertheless, the actual mechanisms of such biological events, involving the sugar head groups of gangliosides, are far from being understood.

Extensive work[7] on ganglioside aqueous solutions, has shown that the bulkyness of their hydrophilic heads dictates their aggregative behavior and that their close packing within their aggregates gives rise to important cooperative behaviors in the hydrophilic layer.[8-15] Surface structural cooperativity could be important in SEDs function. Gangliosides headgroups are able to assume different conformations on the surface of an aggregate, more lying or standing. Switching between different conformations is possible, and is a collective event. Switching has been observed to be induced, in model systems, by concentration or temperature increase, then possibly involving ganglioside-water interaction. Temperature or concentration effects could change the relative interplay of the hydrogen bonding either between water and ganglioside molecules or between sugar units, within the same oligosaccharide chain or belonging to adjacent gangliosides.

This paper reports some new experimental results aimed to probe the effect of the surface transition of ganglioside aggregates on the solvent water. Raman, Depolarized Rayleigh Scattering (DRS), Quasielastic Neutron Scattering (QENS) and high resolution Nuclear Magnetic Resonance (NMR)

experiments reveal that modifications in the water structuring indeed occur for different ganglioside headgroup arrangements. Experiments are performed on micellar model systems, where GM1 headgroups can be packed in either conformation, lying or standing with respect to the aggregate surface.

Materials and Methods

GM1 was extracted and purified as described in Reference (16). A semisynthetic derivative of GM1, namely $GM1_{acetyl}$, carrying the same headgroup of GM1, was obtained from GM1 by substitution of one of the two hydrophobic chains, namely the C18 fatty acid, with the shorter C2 chain.[17] When necessary, the concentration of ganglioside solutions was assessed by standard colorimetric and thin layer chromatography (TLC) methods. For all measurements, ganglioside powder was dissolved in water, freshly double-distilled on a glass apparatus, to the needed final concentration. The resulting micellar solutions were divided in two samples. One was just stored at room temperature (*standing* sample), the second was heated up to 60°C for 30 min before storage (*lying* sample). With this procedure, aggregates hosting GM1 in the two packing conformations are obtained. Aggregates are trapped and stable in the given conformation.

Depolarized Rayleigh Scattering (DRS) experiments. GM1 *standing* and *lying* samples were prepared at a final concentration of 7.5% bw, put in a 5 mm pathlength optical cell and measured at T = 20°C, thermostatted within 0.02°C. Measurements were performed with a double-step double monochromator (SOPRA mod. DMDP2000), with a maximum resolution of 700 MHz. The exciting source was an argon-ion laser operating on the 5145 Å line with a mean power of 300mW. The scattered radiation was collected through a Glan-Thomson polarizer, with an extinction coefficient better than 10^{-7}. Depolarised spectra were measured in the (–100) – (+100) cm^{-1} range.

Raman experiments. Raman-scattering measurements were performed on the same samples, in the same cells, with the same thermostatted bath and with the same exciting source as for DRS experiments. The scattered radiation was collected, through a Glan-Thompson polarizer, onto a

triple-monochromator (Spex Ramalog V) operating with a resolution of 5 cm^{-1}. Spectra were obtained in the range 2800 – 4000 cm^{-1}, both in the polarization parallel (VV) and perpendicular (VH) to the polarization vector of the incident light, which was fixed perpendicular to the optical axis of the interferometer.

Quasielastic Neutron Scattering experiments were performed using the TOFTOF spectrometer at the FRM-II reactor of the Heinz Maier-Leibnitz Zentrum (Munich, Germany). They follow previous ones performed on the same systems at the ILL (Grenoble, France) using the IN5 spectrometer and at ISIS (Chilton, UK) using the IRIS spectrometer (data already published[18,19]). Solutions were prepared by dissolving GM1 in pure D_2O to a final volume fraction of 15%. They were then put into flat quartz cells 50 × 30 mm, 0.5 mm thick. QENS spectra were collected in the *Q*-range 0.2 – 1.2 $Å^{-1}$ with an energy resolution ΔE = 26 μeV (FWHM), close to those of the previous experiments at the ILL and ISIS (20 and 14 μeV respectively). GM1 *standing* and *lying* samples were analysed at 20 °C.

NMR experiments were performed on Bruker AM 500, DRX 500 and DRX 600 MHz spectrometers, the last two equipped with pulsed field gradient system. Bruker XWIN-NMR software was applied for data processing. GM1 and $GM1_{acetyl}$ peak assignment of non-labile protons in D_2O and detectable labile protons in H_2O has been published elsewhere.[20-22] $GM1_{acetyl}$ / water interaction was studied on 10 mM (≈13% bw) *standing* and *lying* samples. Water-protons/headgroup-protons interactions were studied by ^{1}H-NMR pulse sequence based on the WEX II sequence.[23] A selective excitation of water signal, implemented by a 26-28 ms spin echo-filter for T_2 relaxation of the anomeric protons resonating at the same frequency of water, is followed by a mixing period during which magnetization is transferred to headgroup-protons via dipole-dipole interactions or chemical exchange of labile OH and NH.[22] Both NOESY and ROESY versions were performed. Adiabatic Off-resonance ROESY[23,24] was applied varying the θ angle between the static field and the effective field experienced by the nuclei. Measurements were

performed in the temperature range from 3 to 12°C. In fact, rather low temperatures are required for detection of the labile OH and NH signals, that otherwise collapse under the bulk water signal due to the too fast chemical exchange rate.

Results and discussion

Depolarized Rayleigh Scattering experiments. The depolarized light scattered from a medium is due to the fluctuations of the traceless part of the polarizability tensor.[27] For the GM1 micellar solutions, the depolarized scattered intensity, measured in the frequency range – 100 to +100 cm^{-1} around the incident laser frequency, essentially bears information about the collective reorientation of the optically-anisotropic water molecules which are not strictly bound to the micelles. In fact, reorientational motions of the molecules kept together in the micelles are too slow to be resolved in these DRS experiments. At the same time, the contribution of unassociated ganglioside molecules is absolutely negligible, due to their extremely low concentration ($cmc_{GM1} \sim 10^{-8}M$)[7]. In practice the measured DRS spectra can be fitted by a resolution function at low frequency, due to what is too slow to be resolved, plus a Lorentzian line, connected to the exponential decay of local order, plus a constant background connected to higher frequency effects[28]. The physically meaningful parameter of the fit is the half-width at half-maximum (HWHM) of the Lorentzian line of the local-order decay, which relates to the rotational motion of water, governed by the hydrogen-bond (HB) lifetime. The final output is the average water rotational relaxation time τ_W. The fitting procedure is illustrated in Fig.2 for the case of GM1-*standing* solution.

Measurements performed at 20°C give $\tau_W = 1.2 \pm 0.02$ psec and 0.9 ± 0.02 psec, for the *standing* and *lying* samples, respectively. The difference between the two τ_W values is out of experimental errors, evaluated from fits to repeated measurements, and reflects a real physical difference in the dynamics of water in the presence of *standing* or *lying* ganglioside micelles.

But, notably, the two values sit on opposite sides with respect to the literature value[29] of the rotational relaxation time of bulk water at 20°C, 0.98 psec. This indicates that the ganglioside hydrophilic layers of *lying* and *standing* micelles have opposite effects on the surrounding water.

Water in the *standing* micellar solution at 20°C behaves like bulk water at a lower temperature, namely at 5°C. Water is described theoretically as a "dynamic gel" (random network of hydrogen bonds) of "open" water, in which a regular tetrahedral structure exists (directly related to clusters of tetrabonded molecules), and "closed" water, which behaves like a continuum, it being the mixing of all the remaining molecules[30]. As temperature is lowered, water becomes more "open" as clusters increase in number and size. The undercooled behavior of water in the *standing* ganglioside micellar solution suggests that the "open" structure of water is favored by the presence of the dispersed interface of *standing* micelles. The situation is reversed for *lying* micelles: the HB lifetime is shorter with respect to that of bulk water, which means that a more "closed" structure of water is favored by the presence of the dispersed interface of *lying* micelles. The behavior of the *standing* ganglioside micellar solution is similar to what has already been observed for micellar solutions of non-ionic surfactants[31] or for water confined in microporous systems[32] ,an effect that has been ascribed to the hydrophilic nature of the interface. Therefore the surface layer of *lying* micelles seems to be less hydrophilic, as it acts to break the tetra-bonded structure in favor of a more disordered structure of water. This difference in the properties of the *standing* and *lying* micellar interface could be correlated with a different exposure of the sugar rings to water. As a matter of fact, switching from *standing* to *lying* micelles implies a wider average surface per molecule (4%)[11], corresponding to a larger packing parameter.

One could wonder whether the observed effect is connected to the fact that gangliosides are ionic amphiphiles. *Standing* and *lying* micelles could dissociate to a different extent, leading to a different counterion concentration in the surrounding water[33]. This is not the case, as it has been verified by small angle neutron scattering measurements, performed on the PAXE instrument at LLB (Saclay-France). Following the same procedure described in reference[34] on solutions in the same range of

concentration as in the DRS measurements, *standing* and *lying* micelles have been tested to bear the same fractional charge (10%), that is, to release in solution the same number of Na^+ counterions per mole.

It has to be noted that the ganglioside solutions are semi-dilute, 7.5% bw corresponding to a GM1 volume fraction $\Phi = 0.061$. The average volumes of the *standing* and *lying* micelles are roughly $6x10^5Å^3$ and $4x10^5Å^3$, respectively. Then the average volumes available per micelle in the solution are roughly $99 \times 10^5Å^3$ and $66 \times 10^5Å^3$. This corresponds to an average center-to-center distance of $(2\times215) = 430$ Å and $(2\times187) = 374$ Å, eight times the micellar radius, and to an average surface-to-surface distance of 326 Å and 284 Å, allowing for more than 80 and 70 water layers, on average, in the intermicellar space. Then, a large amount of bulk water surrounds the micelles. Only a fraction of the order of 1-2% of the total water volume can be estimated to participate to a 4 Å-shell close to the micelle surface. The clear visibility of the effect (of the order of 20% and 10%) forcedly suggests that the influence of the sugar interface on the coordination of water molecules extends over much longer distances than expected.

Raman scattering experiments. An independent check, supporting DRS results, comes from the Raman scattering data, obtained on the same samples at the same temperature, 20°C. Fig. 3 shows the Raman spectra for the *standing* and *lying* ganglioside micellar solutions, measured in the range 2900–3600 cm^{-1}. The spectrum of pure water is drawn for comparison. Intensities have been normalized to spectral areas and concentration. Fig. 3 reports the isotropic part of the scattered intensity $I_{IS}(w) = I_{VV}(w) - (4/3)I_{VH}(w)$ which is connected to the molecular vibrations[27] and, in particular for the present measurements, to the OH-stretching (OHS) mode of water. $I_{VV}(w)$ and $I_{VH}(w)$ refer to the (VV) and (VH) contributions to the scattered intensity.

With the nomenclature of the above mentioned theoretical model,[30] which describes water as a "dynamic gel", both "open" and "closed" water contribute to the OHS vibrational spectrum, in two different frequency regions. The "open" contribution has a mean peak located at 3150 cm^{-1}, while the "closed" peak is centred at 3500 cm^{-1} [35] .Indeed, it can be seen from Fig.3 that the *standing*

ganglioside micellar solution gives rise to a higher "open" peak and a lower "closed" peak as compared to the ones of bulk water. The *lying* solution behaves in the opposite way. Thus, also Raman data confirm the argument based on the DRS measurements that the dispersed interface of *standing* micelles favours the "open" structure of water, while the *lying* favours the "closed" one.

Quasielastic Neutron Scattering experiments. First neutron experiments carried out by us indicated that the presence of GM1 micelles slows down the dynamics of the solvent with respect to that of pure water[18] and allowed us to determine the diffusive dynamics of GM1 hydrogens [19]. The aim of the present experiment was to make a comparison of GM1 samples in *standing* and *lying* configuration in D_2O buffer. Owing to the different incoherent neutron scattering length of hydrogen and deuterium, the buffer and micelle subspectra have comparable intensities and can be clearly distinguished (see Fig. 5 in the following). In order to compare the present data to the previous ones, we have adopted the same simplified model used previously[18,19] for the dynamical structure factor:

$$S_{tot}(Q,\omega) = e^{-Q^2\langle u^2\rangle/3}\left[A_{gan}S_{gan}(Q,\omega) + (1-A_{gan})S_{buf}(Q,\omega)\right] + B \qquad (1)$$

Here a common Debye-Waller factor ($e^{-Q^2\langle u^2\rangle/3}$) takes into account fast vibrational motions, *Agan* is the scattering intensity from gangliosides and from the closely associated water shell, *B* is a flat instrumental background. The GM1 contribution, $S_{gan}(Q,\omega)$, is described in terms of a confined diffusive motion; it is then convoluted to a Lorentzian $L_{CM}(Q,\omega)$, that describes the Brownian diffusion of the micelle as a whole[36]

$$S_{gan}(Q,\omega) = \left[A_0(Q)\delta(\omega) + (1-A_0(Q))L_{gan}(Q,\omega)\right] \otimes L_{CM}(Q,\omega) \qquad (2)$$

$A_0(Q)$ is the incoherent structure factor, EISF, and $L_{gan}(Q,\omega)$ is a quasielastic component described by a single Lorentzian term. For the scattering law of the buffer we adopted a simple phenomenological model already used to describe QENS from pure supercooled water[37]:

$$S_{buf}(Q,\omega) = \left[A_1(Q)L_1(Q,\omega) + (1-A_1(Q))L_2(Q,\omega)\right]$$

It contains two Lorentzian components: a narrow one , L_1, with weight $A_1(Q)$ that describes the slow relaxation processes corresponding to the long range translational diffusion, and a broad one, L_2, that accounts for the local dynamics of water molecules inside the cage formed by the nearest neighbors. The total scattering law has then been convoluted to the instrumental resolution function. In all the fits, the diffusion coefficient of the micelles that determines the width of $L_{CM}(Q,\omega)$ was kept fixed to the value $D_0 = 1.8 \times 10^{-7}$ cm^2 s^{-1} deduced from the hydrodynamic radius of the micelles. Fig. 3 shows a comparison of the raw neutron spectra, at the same temperature (20°C) and Q-value, for GM1 samples in the *standing* and *lying* configurations; the difference is small but clearly visible owing to the excellent noise to background ratio of TOFTOF, and to the high counting statistics of the spectra. In Fig. 4 a typical QENS spectrum for a 15% GM1 *lying* sample in D_2O buffer is shown: the quasielastic subspectrum due to GM1 is much narrower than that of the D_2O buffer, and these two components can be easily singled out. For the confined dynamics of GM1 hydrogens we adopted the simple Volino-Dianoux model of a free diffusion within a sphere with rigid walls[38].

From the Q-dependence of the EISF ($A_0(Q)$ in eq. 2) and from that of the quasielastic Lorentzian, L_{gan}, we could estimate the radius of the volume explored by the protons, a, and the diffusion coefficient within the confining sphere, D_{gan}. In going from the *lying* to the *standing* configuration, the former decreases from 2.8 to 2.4 Å; at the same time D_{gan} decreases from 2.2×10^{-5} cm^{2}s^{-1} (*lying*) to 1.6×10^{-5} cm^{2}s^{-1} (*standing*).

The different configurations of the GM1 head groups affect also buffer dynamics. In the analysed Q-range ($Q_{max} \sim 1.2$ Å^{-1}, which is well below the first maximum of D_2O structure factor), H_2O and D_2O QENS spectra show similar translational broadenings, with a reduction of the measured diffusion coefficient of about 18% in going from H_2O to D_2O that arises from mass difference.

The Q-dependence of the diffusive broadening, $\Gamma_{trans}(Q)$, of the L_1 Lorentzian component that accounts for long-range translational diffusion, was analysed in terms of a random jump model[39] that gives:

$$\Gamma_{trans}(Q) = \frac{D_t Q^2}{1 + D_t Q^2 \tau_0}$$

Where D_t is the self-diffusion translational coefficient and τ_0 is the residence time between subsequent jumps. Fig. 6 shows the dependence upon Q^2 of $\Gamma_{trans}(Q)$ for pure D_2O, and for the buffer components of the *standing* – and *lying*-GM1 spectra. The fit is quite good in the three cases reported, and it provides decreasing values of D_t from 1.92×10^{-5} cm^2s^{-1} (pure D_2O) to 1.68×10^{-5} cm^2s^{-1} (*lying* GM1 buffer) and to 1.61×10^{-5} cm^2s^{-1} (*standing* GM1 buffer). At the same time, the residence time τ_0 increases slightly from 1.37 ps (pure D_2O) to 1.56 ps (*lying* sample) and 1.63 ps (*standing* sample). We obtain therefore a 16% reduction of diffusivity with respect to pure water in the case of the *standing* GM1 buffer and a 12.5% reduction in the case of the *lying* one. These data support the DRS and Raman results confirming the existence of a difference in the dynamics of water in the presence of *standing* or *lying* ganglioside micelles. The fact that the dynamics of GM1 hydrogens is slow, on the other hand, is not surprising: it can be related to the rather close packing of the bulky sugar headgroups in the hydrophilic shell of the micelle.

NMR experiments. NMR is known to be a powerful tool to study conformations and interactions on the Ängstrom scale. It is therefore useful to gain additional independent information on the interfacial properties of *standing* and *lying* ganglioside aggregates. In order to keep the aggregated structures small enough for NMR investigation, $GM1_{acetyl}$ derivative was used. $GM1_{acetyl}$ carries the same headgroup of GM1, but one of the two hydrophobic chains is shorter, so it forms small micelles, with an average aggregation number of 76 and a molecular weight of 102.000.[17] Its micelle size is small enough, so that high resolution NMR spectroscopy can still be performed without great loss of resolution. In fact, for $GM1_{acetyl}$ micelles, in the temperature range from 3 to 12°C, the characteristic time of water-/sugar-protons interaction falls in the tenth-of-millisecond range.

A complete study of the *standing* $GM1_{acetyl}$ headgroup spatial interaction has already been published.[17] In the present experiments we find that the H^1-H^1 interaction networks are essentially

the same for *standing* and *lying* micelles, that is, they do not reveal any modification for what concerns the *internal* conformation of the headgroup, i.e., the mutual disposition of the sugar groups within the headgroup, at least within the 4Å-length-scale.

In addition to this conformational assessment, a pulse sequence aimed to measure the magnetization transfer from selectively excited water-protons to sugar-headgroup-protons, was applied (see Methods section). Water selective 1D-NOESY and ROESY experiments have been performed. During these measurements, the non labile proton magnetization transfer is determined by two competing phenomena: the direct dipole-dipole interaction and the interaction mediated by chemical exchange through the labile OH and NH protons of the ganglioside (17 all over the headgroup). The possibility to distinguish between these effects was an essential point in this study[40]. The importance of the chemical exchange processes was tested by means of off-resonance adiabatic ROESY, with the ϑ angle between the external magnetic field and the effective field felt by the spin system fixed to 35.3°.[41] In fact, in this experimental configuration, all contributions to the cross-relaxation but the chemical exchange are suppressed (see Fig.7). The study of the NOE and ROE buildup curves indicates that, for the generality of the ganglioside protons, the interaction with water is strongly mediated by chemical exchange with OH. In the following, we report results obtained for three free OH's in the spectrum, corresponding to the three OH's marked in Fig.1, which are not affected by spectral overlapping that prevents safe analysis.

With this experimental approach we investigated whether any alteration of the hydrated shell of the aggregate hosting GM1 headgroups is brought about by the *standing* to *lying* switch.

Fig.8 reports the magnetization buildup curves, obtained by 35.3°-ROESY, for the three OH's marked in Fig.1, relative to the *standing* and *lying* samples, measured at 12°C. It can be seen that, in all cases, buildup is completed in shorter times for *lying* samples, indicating a higher rate of exchange for all the three investigated OH's in the *lying* state.

Fig.9 reports the characteristic times of magnetization buildup for the three mentioned OH's obtained by 1D-NOESY experiments, performed on *standing* and *lying* samples at three different

temperatures, namely 3°C, 7°C and 12°C. As previously discussed, the reported results are expressed in terms of time of exchange, water/OH exchange being the main contribution to the transfer. Again the *lying* OH's show a higher NOE rate, in agreement with 35.3°-ROESY results.

It is interesting to notice that the set of data relative to the NeuAcOH8 group of the branched sialic acid (see Fig.1 for proton location in the molecular structure), belonging to the *standing* system, has an abrupt increment of the time of exchange at the lowest temperature (3°C). This corresponds to high activation energy for the exchange process, indicating that this OH-group is strongly engaged in other interactions, possibly in hydrogen-bonding with the carboxylic group of the sialic acid itself. This has also been suggested for the GM1 unassociated monomers dissolved in non-water solvents.[20] The present result indicates that the same engagement is active also when GM1 headgroup is inserted in an aggregated structure. In *lying* micelles this intramolecular interaction appears to be sensibly weakened, as indicated by the reduction of the buildup time by a factor of two. Looking back to Fig.5, it can be seen that also the 35.3°-ROESY results show a peculiar behavior of NeuAcOH8 as compared to the other OH's, consisting in an inversion in intensity between *standing* and *lying* samples. Also this effect could be explained by invoking a reduced availability of this group for the chemical exchange process, in *standing* micelles, being already engaged in a different interaction. Moreover, the large difference in intensity between *standing* and *lying* signals belonging to the GalOH2 indicates that in this region, deeply embedded in the hydrophilic shell, water/OH exchange takes place at very different rates in *standing* and *lying* micelles. Nevertheless, apart from the specific considerations on the single OH's, the general behaviour of an increased exchange rate for *lying* micelles could be explained in terms of a longer residence time of water molecules in the hydration shell as compared to the *standing* ones.

Therefore, NMR measurements point out that the collective packing switch induces irreversible local modifications in the headgroup-environment interaction.

Conclusions

Depolarized Rayleigh Scattering, Raman Scattering, Quasielastic Neutron Scattering and NMR measurements performed on GM1 ganglioside solutions indicate that both the structural properties of solvent water and its interactions with the sugar headgroups of gangliosides are modified by the collective surface remodeling of the headgroups. The extent of this modification is much higher than expected. Within the Stillinger and Weber model of inherent structures, this modification can be seen as a change of the relative proportion of open and closed water. In a biological perspective, water structure modulation could be one of the physico-chemical elements contributing to the raft strategy. Moreover, this would reinforce the comparison in complexity between ganglioside assemblies and proteins, the structure and functionality of which is known to be involved in an interplay with the solvent structure.

Aknowledgements

We thank Patrick Berthault for his precious help in performing NMR experiments, as well as Norberto Micali for his skilled assistance in DRS measurements.

The small-angle neutron scattering measurements used in the present paper were performed on the PAXE instrument at LLB (Saclay-France).

REFERENCES

1) Tettamanti, G.; Sonnino, S.; Ghidoni, R.; Masserini, M.; Venerando, B. **1985,** In *Physics of Amphiphiles. Micelles, Vesicles and Microemulsions*; Degiorgio, V. and Corti, M., Eds.; North Holland, Amsterdam, p.607.
2) Simons, K.; Ikonen, E. *Nature* **1997**, 387, 569-572.
3) Nagai, Y. *Pure Appl.Chem.* **1998,** 70, 533-538 ; Lloyd, K.O.; Furukawa, K. *Glyconj.J.* **1998,** 15, 627-636.
4) Hakomori, S.I.; Handa, K.; Iwabuchi, K.; S. Yamamura; Prinetti A. *Glycobiology* **1998,** 8, XI-XIX.
5) Hakomori, S.I. *Glyconj.J.* **2000**, 17, 143-151.
6) K. Kasahara; Sanai Y. *Glyconj.J.* **2000,** 17, 153-162.
7) Sonnino, S.; Cantu', L.; Corti, M.; Acquotti, D.; Venerando B. *Chem.Phys.Lipids* **1994,** 71, 21-45.
8) Cantu', L.; Corti, M.; Del Favero, E.; Digirolamo, E.; Sonnino. S.; Tettamanti, G. *Chem.Phys. Lipids* **1996,** 79, 137-145.
9) Boretta, M.; Cantu', L.; Corti, M.; Del Favero, E. *Physica A* **1997,** 236, 162-176.
10) Corti, M.; Boretta, M.; Cantu', L.; Del Favero, E.; Lesieur, P. *J.Molec.Structure* **1996,** 383, 91-98.
11) Cantu', L.; Corti, M.; Del Favero, E.; Digirolamo, E.; Raudino, A. *J.Phys.II (France)* **1996,** 6, 1067-1090.
12) Cantu', L.; Corti, M.; Del Favero, E.; Muller, E.; Raudino, A.; Sonnino, S. *Langmuir* **1999**, 15, 4975-4980.
13) Cantu', L.; Corti, M.; Del Favero, E.; Raudino, A. *J.Phys.Condens. Matter* **2000,** 12, 321-325.
14) Cantu', L.; Corti, M.; Del Favero, E.; Raudino, A. *Langmuir* **2000,** 16, 8903-8811.
15) Cantu', L.; Corti, M; Sonnino S.; Tettamanti G. *Chem.Phys. Lipids* **1986,** 41, 315-328.
16) Tettamanti G.; Bonali, F.; Marchesini, S.; Zambotti, V. *Biochim.Biophys. Acta* **1973,** 296, 160-170.
17) Sonnino, S.; Cantu', L.; Corti, M.; Acquotti, D.; Kirschner G.; Tettamanti G. C*hem.Phys. Lipids* **1990,** 56, 49-57.
18) Cantù L.; Cavatorta F.; Corti, M.; Del Favero, E.; Deriu, A. *Physica B* **1997**, 234-236, 281-282.
19) Brocca, P.; Cantù L.; Cavatorta F.; Corti, M.; Del Favero, E.; Deriu, A.; Di Bari M. *Physica B* **2004**, 350, e619-e622.
20) Acquotti, D.; Poppe, L., Dabrowski, J.; von der Lieth, C. W.; Sonnino, S.; Tettamanti, G. *J.Am.Chem.Soc.* **1990,** 112, 7772-7778.
21) Brocca, P.; Cantu', L.; Sonnino S. *Chem.Phys. Lipids*. **1995,** 77, 41-49.
22) Brocca, P.; Berthault, P.; Sonnino, S. *Biophys.J.* **1998,** 74, 309-318.
23) Mori, S.; Berg, J.M.; van Zijl, P.C.M. *J.Biomol.NMR*. **1996,** 7, 77-82.
24) Desvaux, H.; Berthault, P.; Birlirakis, N.; Goldman, M. *J.Mag.Reson. A.* **1994,** 108, 219-229.
25) Desvaux, H.; Berthault, P.; Birlirakis, N.; Goldman, M.; Piotto, M. *J.Mag.Reson. A.* **1995,** 113, 47-52.
26) Kauppinen, J.K.; Moffatt, D.J.; Mantsch, H.H.; Cameron, D.G. *Applied Spectroscopy* **1981,** 35, 271-276.
27) Berne, B.J.; Pecora, R., *Dynamic Light Scattering*, Wiley, New York, 1976.
28) Aliotta, F.; Vasi, C.; Malsano, G.; Majolino, D.; Mallamace, F.; Migliardo, P., *J.Chem.Phys.* **1986,** 84, 4731-4738.
29) Montuose, C.J.; Bucaro, J.A.; Marshall-Coaklleym, J.; Litovitz, T.A. *J.Chem.Phys.* **1974,** 60, 5025- ; Conde, O.; Texeira, J., *J.Phys. (France)* **1983**, 44, 525-529.
30) Texeira, J.; Stanley, H.E. *J.Chem.Phys.* **1980**, 73, 3404- . Angell, C.A. **1982,** In *Water: a Comprehensive Treatise;* Franks, F., Ed.; Vol.7, pp 1-81, Plenum, New York.

31) Mallamace, F.; Earnshaw, J.C.; Micali, N.; Trusso, S.; Vasi, C., *Physica A* **1996**, 231, 207-.
32) Zanotti, J. M.; Bellissent-Funel, M.C.; Chen, S.H., *Phys.Rev.E* **1999,** 59, 3084-3093.
33) Micali, N.; Vasi, C.; Mallamace, F.; Corti, M.; Degiorgio, V., *Phys.Rev.E* **1993,** 48, 3661-3666.
34) Degiorgio, V.; Cantu', L.; Corti, M.; Piazza, R.; Rennie, A. *Coll.Surf.* **1989,** 38, 169-178.
35) D'Arrigo, G.; Maisano, G.; Mallamace, F.; Migliardo, P.; Wanderlingh, F., *J.Chem.Phys.* **1981,** 4264-4270.
36) Perez, J.; Zanotti, J-M.; Durand, D. *Biophys. J.* **1999**, 77, 454.
37) Di Cola, D.; Deriu, A.; Sampoli, M.; Torcini, A. *J. Chem. Phys.* **1996**, 104, 4223.
38) Volino, F.; Dianoux, A.J. *Mol. Phys*., **1980**, 41, 271.
39) Teixeira J., Bellissent-Funel M.-C., Chen, S.H., Dianoux, A.J. *Phys. Rev. A*, **1985**, 31, 1913.
40) Positive NOE and all ROE cross peaks have opposite sign with respect to the excited water signal, while chemical exchange ones have the same sign. A combination of chemical exchange-ROE transfer gives rise again to cross peaks of opposite sign.
41) Brocca, P.; Berthault, P.; Sonnino, S. *Biophys.J.* **1998**, 74, 309-318.

FIGURE CAPTIONS

Figure 1. Chemical structure of GM1 ganglioside. Ceramide, the lipid moiety, is constituted by two hydrophobic chains, a long chain amino alcohol (sphingosine, Sph), and a fatty acid connected to it by an amide linkage. GM1 has a four-sugar backbone, namely the Glc (glucose) - Gal (galactose) - GalNAc (N-acetylgalactosamine) - Gal (galactose) and a sialic acid NeuAc (N-acetylneuraminic acid) branched to the internal Gal. Shadowing indicates the position of the GM1 OH's followed by NMR in their exchange with hydration water.

Figure 2. Spectrum analysis of DRS experiment on *standing* GM1 solution. The continuous line represents the best fit with the three contributions: instrumental resolution (full line), physically significative Lorentzian (dot-dash line) and background (dotted line).

Figure 3. Raman spectra for the *standing* and *lying* ganglioside micellar solutions, as compared to that of pure water at the same temperature.

Figure 4. Comparison of the raw neutron spectra for *standing* and *lying* GM1 samples at the same temperature and *Q*-value. The log scale evidences the differences that extend all over the tails of the QENS curves and therefore affect both micelle and buffer subspectra.

Figure 5. QENS spectrum at Q = 1 $Å^{-1}$ for a 15% GM1 (*lying* configuration) micellar solution in D_2O at 20°C. The total fit as well as the components due to the ganglioside (I_{EL} and I_{QE}) and to the buffer (continuous line: slow relaxation, and dashed line: fast relaxation) are reported.

Figure 6. *Q*-dependence of the broadening of the translational diffusion component of the D*2*O buffer. Pure D*2*O data (triangles) are compared to those of the buffers for *standing* (squares) and *lying* (circles) GM1 samples. The continuous lines are fits to the random jump diffusion model described in the text.

Figure 7. ^{1}H-NMR spectra of $GM1_{acetyl}$ micellar solution obtained by selective excitation of the water signal. NOESY, ROESY, and ROESY-35.3° versions are reported, all taken at 120 ms mixing time. In the ROESY-35.3° spectrum, the CH signals on the right hand side of the suppressed

water are missing, as in these experimental conditions the dipole-dipole magnetization transfer is prevented. On the contrary, the OH signals on the left hand side are present, due to the occurrence of chemical exchange between OH's and water protons. The OH region is quite similar in the three spectra, with comparable intensities, clearly indicating that chemical exchange is the dominant phenomenon in the magnetization transfer, even when dipole-dipole transfer is allowed. ROE from OH to CH (opposite sign) and NOE from OH to CH (same sign) cause the enhancement of the signals in the CH region of the ROESY and NOESY spectra, respectively.

Figure 8. Magnetization buildup curves, obtained by 35.3°-ROESY, for the three OH's marked in Fig.1, relative to the *standing* (open symbols) and *lying* (full symbols) samples, measured at 12°C. Apart from signal intensity, the buildup characteristic times are uniformly shorter for the *lying* solution.

Figure 9. Characteristic times of magnetization buildup for the three mentioned GalOH2 (diamonds), NeuAcOH8 (circles) and NeuAcOH4 (squares), obtained by 1D-NOESY experiments, performed on *standing* (open symbols) and *lying* (full symbols) micelles at three different temperatures, of 3°C, 7°C and 12°C. Lines are drawn to guide the eye. The arrow evidences the strong decrease of exchange time in the case of NeuAcOH8 passing from *standing* to *lying* solution.

Fig.1

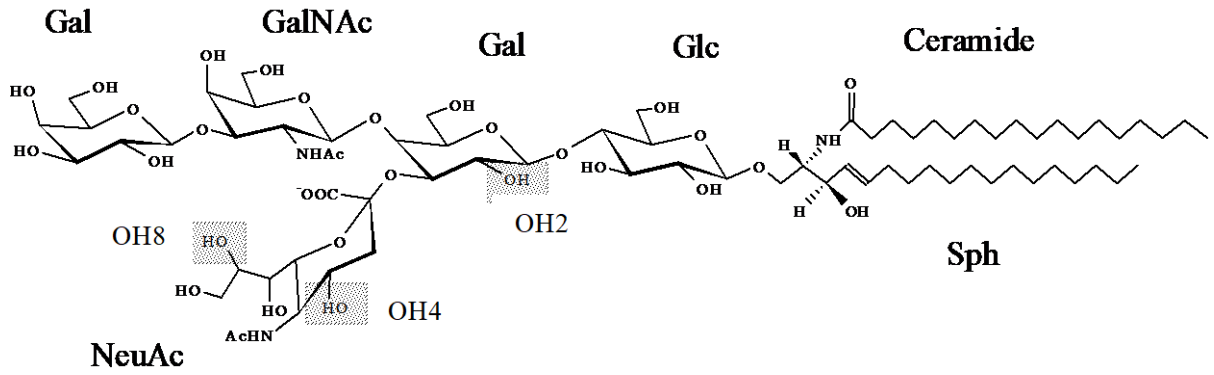

Fig.2

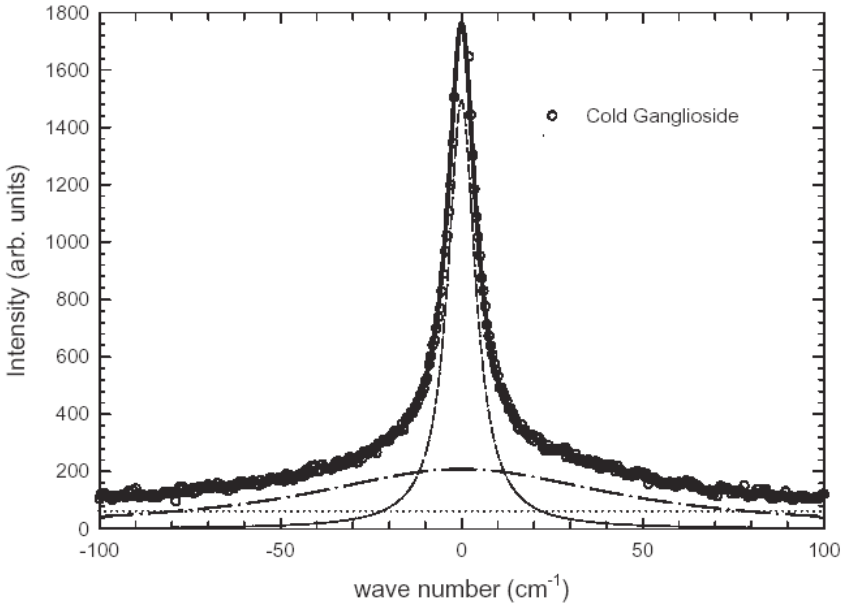
Cold Ganglioside
Intensity (arb. units)
wave number (cm-1)
1800
1600
1400
1200
1000
800
600
400
200
0
-100
-50
0
50
100

Fig.3.

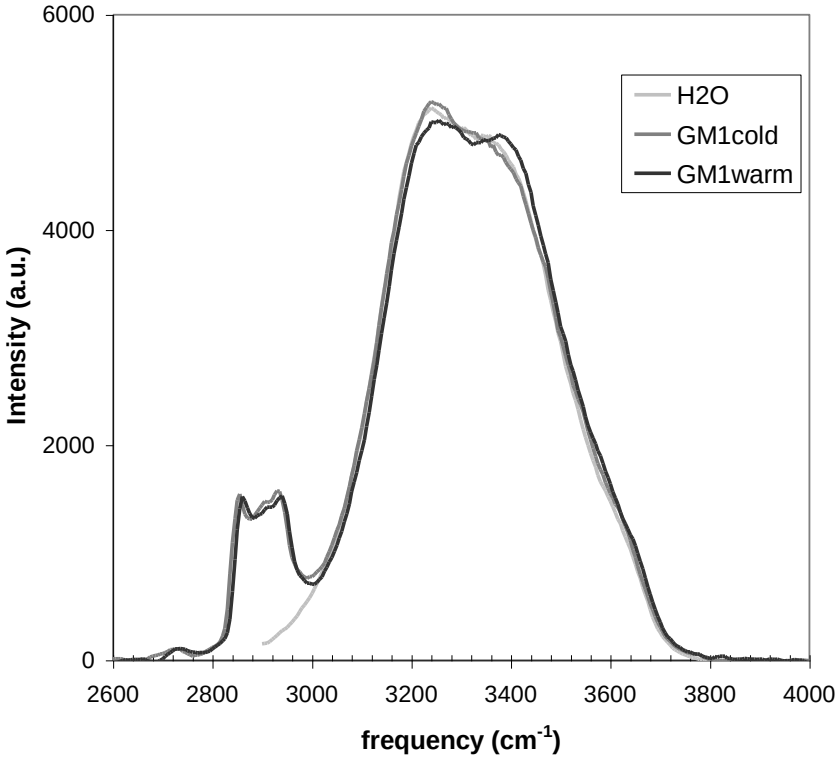
6000
4000
2000
0
Intensity (a.u.)
2600
2800
3000
3200
3400
3600
3800
4000
frequency (cm-1)
H2O
GM1cold
GM1warm

Fig. 4

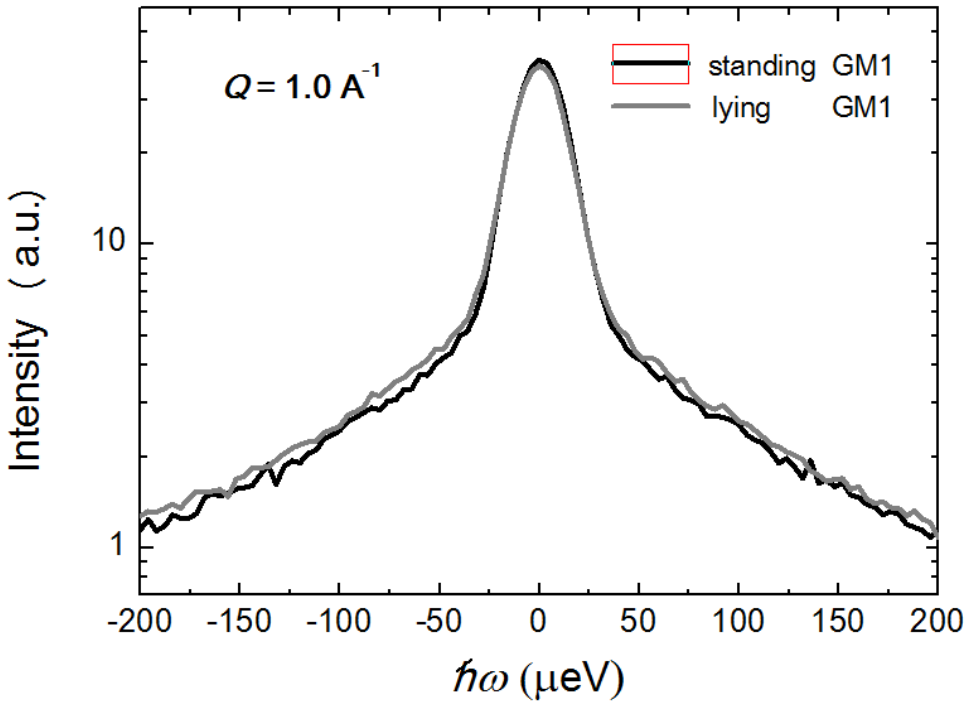
Q = 1.0 A-1
standing GM1
lying GM1
Intensity (a.u.)
10
1
-200
-150
-100
-50
0
50
100
150
200
ħω (μeV)

Fig. 5

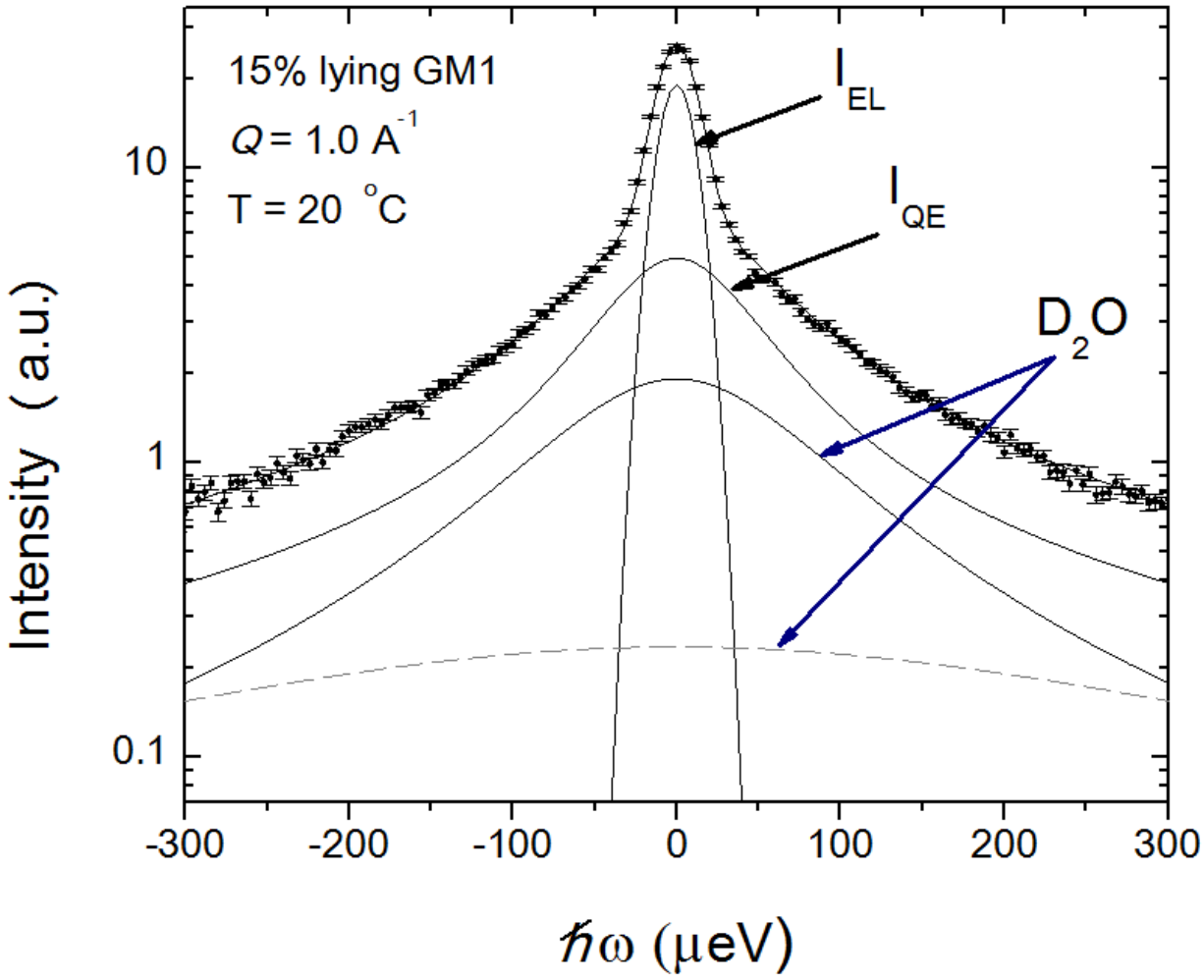
15% lying GM1
Q = 1.0 A-1
T = 20 °C
I EL
I QE
D2O
Intensity (a.u.)
10
1
0.1
-300
-200
-100
0
100
200
300
ħω (μeV)

Fig.6

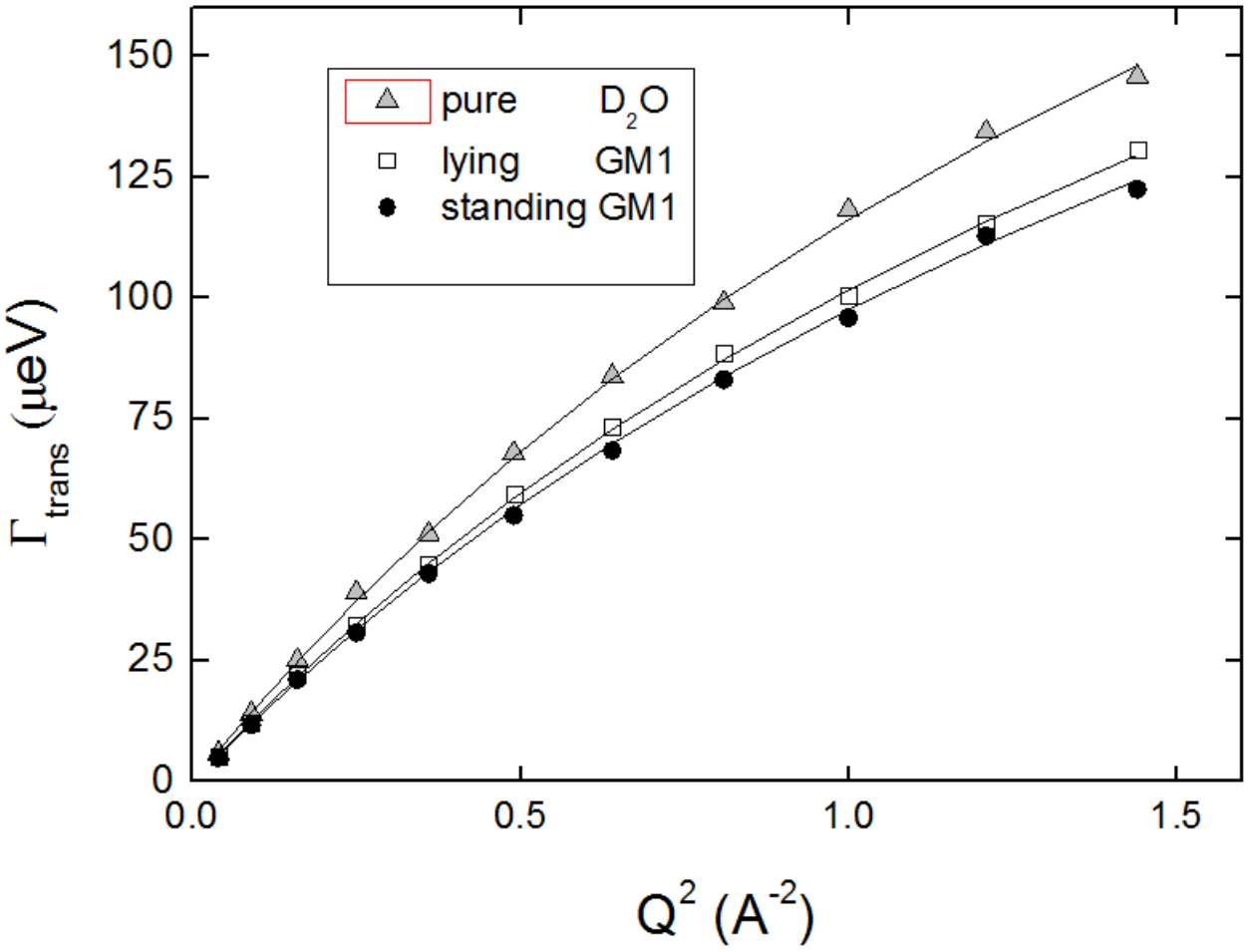
pure D2O
lying GM1
standing GM1
Γtrans (μeV)
Q2 (A-2)
0
25
50
75
100
125
150
0.0
0.5
1.0
1.5

Fig. 7

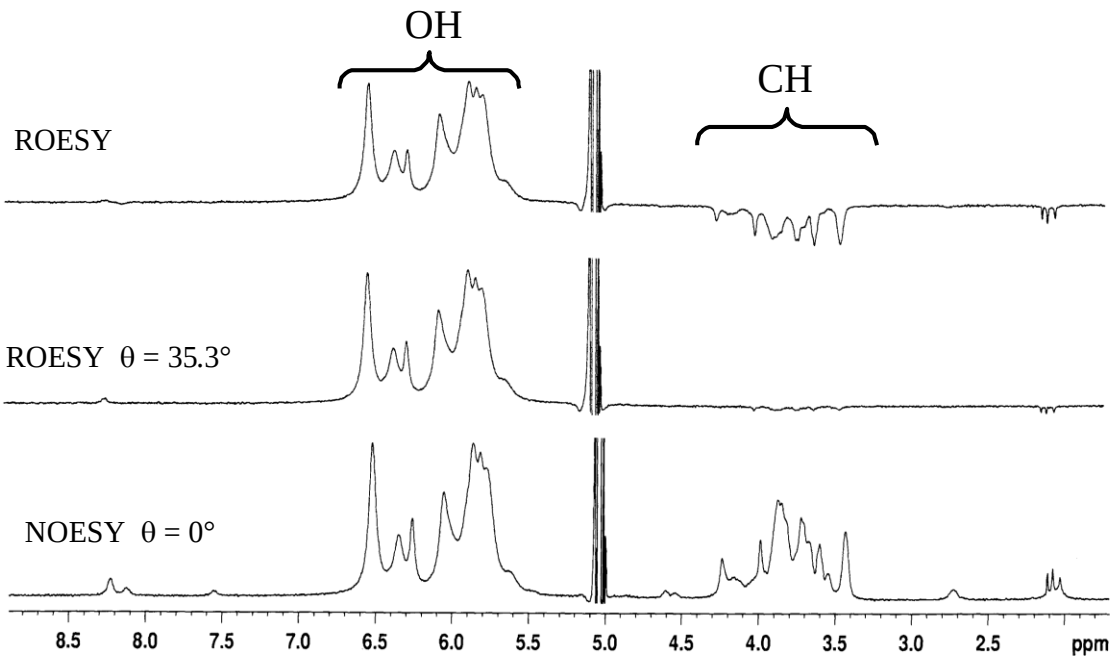
OH
CH
ROESY
ROESY θ = 35.3°
NOESY θ = 0°
8.5
8.0
7.5
7.0
6.5
6.0
5.5
5.0
4.5
4.0
3.5
3.0
2.5
ppm

Fig.8

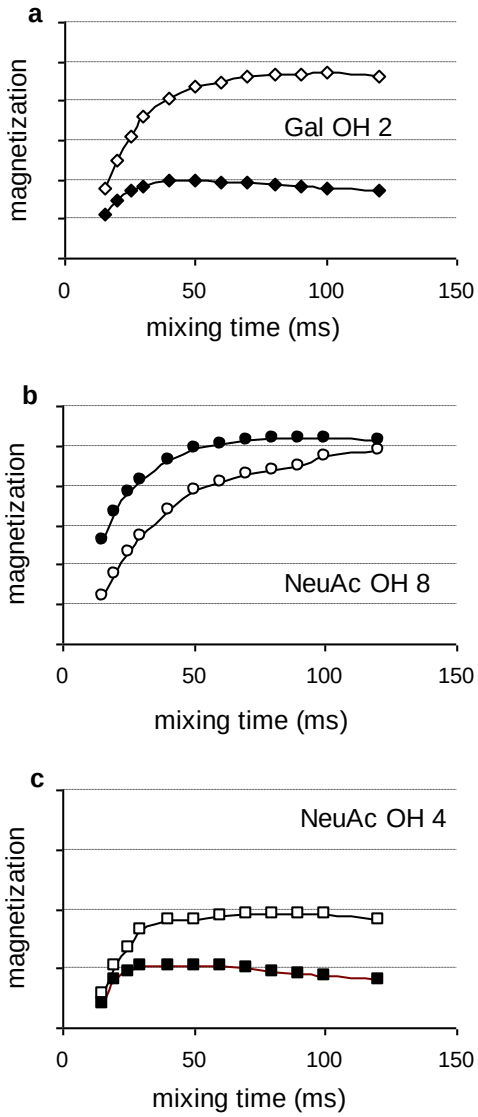
a
magnetization
Gal OH 2
0
50
100
150
mixing time (ms)
b
magnetization
NeuAc OH 8
0
50
100
150
mixing time (ms)
c
magnetization
NeuAc OH 4
0
50
100
150
mixing time (ms)

Fig.9

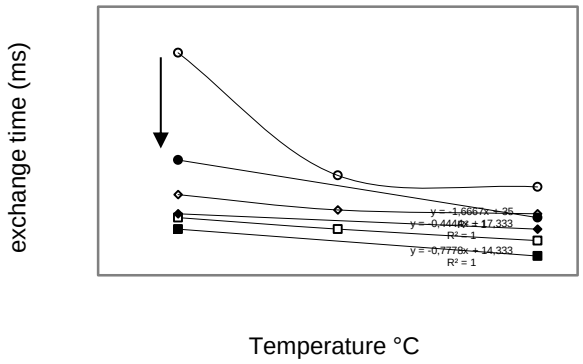
exchange time (ms)
y = -1,6667x + 35
R² = 1
y = -0,4444x + 17,333
R² = 1
y = -0,7778x + 14,333
R² = 1
Temperature °C

TOC IMAGE